Presented at 6th EARSeL SIG IS Workshop, March 16-18, 2009, Tel Aviv, Israel

A NEW LABORATORY FOR THE CHARACTERISATION OF HYPERSPECTRAL AIRBORNE SENSORS

P. Gege[a,*], J. Fries[a], P. Haschberger[a], P. Schötz[a], B. Suhr[a], W. Vreeling[a], H. Schwarzer[b], P. Strobl[c], G. Ulbrich[d]

[a]DLR, Remote Sensing Technology Institute, Oberpfaffenhofen, D-82234 Wessling, Germany – (peter.gege, jochen.fries, peter.haschberger, paul.schoetz, willem.vreeling) @ dlr.de
[b]DLR, Optical Information Systems, Rutherfordstr. 2, D-12489 Berlin, Germany – horst.schwarzer@dlr.de
[c]European Commission, Joint Research Center, Inst. for Environment and Sustainability, I-21023 Ispra, Italy – peter.strobl@jrc.it
[d]European Space Agency (ESA), Keplerlaan 1, NL-2200 AG Noordwijk, The Netherlands – Gerd.Ulbrich@esa.int

KEY WORDS: Calibration, laboratory, hyperspectral, imaging spectrometer, APEX.

ABSTRACT:

A new facility designed to characterize the spectral, radiometric and geometric properties of hyperspectral airborne sensors was established at the German Aerospace Center (DLR) in Oberpfaffenhofen. This laboratory will serve as Calibration Home Base (CHB) for the airborne imaging spectrometer APEX (Airborne Prism Experiment), which is currently being developed under the authority of the European Space Agency (ESA). In APEX configuration (wavelength range: 380 to 2500 nm, instantaneous field of view: 0.48 mrad, field of view: ±14°) spectral measurements can be performed to a wavelength uncertainty of ±0.15 nm, geometric measurements at increments of 0.0017 mrad across track and 0.0076 mrad along track, and radiometric measurements to an uncertainty of ±3 % relative to national standard. Computer control of major laboratory equipment allows automation of time consuming measurements. The facility can be adapted to similar sensors including such with thermal infrared detectors.

1. INTROCUCTION

The Calibration Home Base (CHB) is a new optical laboratory for the calibration of airborne hyperspectral sensors and field spectrometers. It is operational since 2007. A photo is shown in Figure 1.

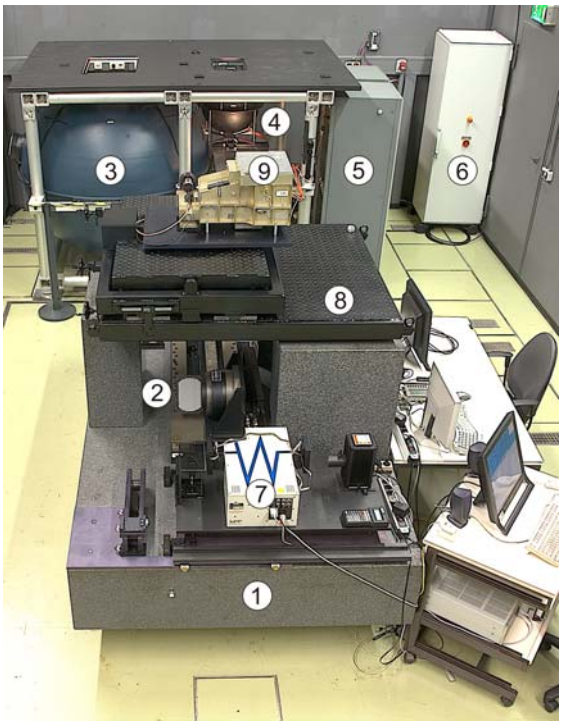

Figure 1. CHB components. 1 = Optical bench, 2 = Folding mirror, 3 = Large integrating sphere, 4 = Small integrating sphere, 5 = Rack with power supplies for 18 lamps of No. 3, 6 = Control electronics for No. 2, 7 = Monochromator, 8 = Mechanical interface, 9 = Sensor (ROSIS).

The CHB was partly funded by ESA to establish a calibration facility for the airborne imaging spectrometer APEX (Itten et al. 2008), but is used for other optical sensors as well. It is the only facility in Europe which allows precise characterisation of the radiometric, geometric and spectral properties of bulky and heavy instruments up to 500 kg (including mechanical interface) in a wide spectral range from 380 nm to 14 µm (Gege et al. 2009).

2. PREMISES

The CHB is located close to DLR's airfield in Oberpfaffenhofen and accessible to bulky instruments. It is installed in a large room (12.8 x 9.0 m², 8 m height). A crane is mounted on the ceiling for handling of heavy components. The room can be darkened. An air condition keeps the temperature at 22 ± 1 °C. Relevant environmental parameters (temperature, pressure, humidity, ambient light) are monitored and included automatically to each measurement protocol.

3. FOLDING MIRROR CONCEPT

A folding mirror design facilitates angle-dependent geometric and spectral measurements of heavy instruments. The set-up is shown in Figure 2. The sensor is mounted on a massive optical bench using a mechanical interface which allows alignment of the sensor's along track position and its yaw and pitch angles. After alignment, the sensor is kept in fixed position downward looking like in the airplane. A flat mirror (12 x 18 cm²) reflects the beam at a well-defined angle (±0.007 mrad uncertainty) to the sensor aperture. This 'folding mirror' can be tilted in order to align the sensor's roll angle and to set the angle of incidence during a measurement, and it can be moved in horizontal direction (±37 cm) to adjust the across track position to the current incident angle in order to meet the entrance aperture.

*Corresponding author.

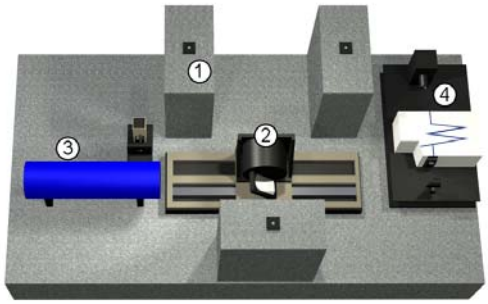

Figure 2. Folding mirror set-up. 1 = Pillar bearing the instrument, 2 = folding mirror, 3 = assembly for geometric measurements, 4 = assembly for spectral measurements.

4. FLAT-FIELD MEASUREMENTS

The sensitivity of imaging sensors is usually not constant across the field of view due to response differences of individual pixels, variations of the entrance slit width, and vignetting of optical components. Figure 3 shows such sensitivity variation at the example of the imaging spectrometer AISA (Kuhlbach 2008). The sensor's field of view was illuminated homogeneously using the CHB's small integrating sphere. The plot shows the dark current corrected signals of AISA's 364 pixels for 4 spectral channels, normalized to the channel's average signal. In this case sensitivity changes about ± 10 % across the field of view, and the effect is wavelength independent.

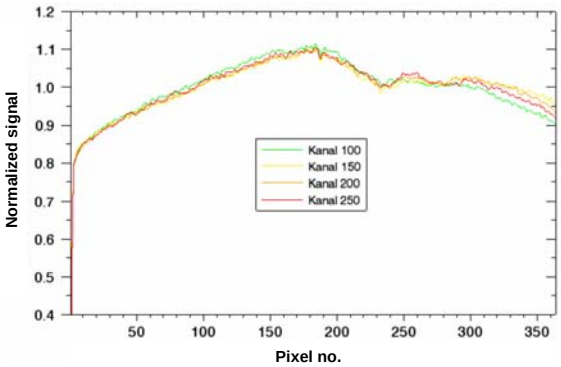

Figure 3: Example of a flat-field measurement (Kuhlbach 2008).

In particular for instruments with large aperture or large field of view, a large integrating sphere (1.65 m diameter) is available to measure these variations quantitatively. The sphere is illuminated from the interior by up to 18 stabilised lamps and provides very homogeneous radiance for an area of 55 x 40 cm² (variations <0.5 % rms). The radiant exitance can be changed from 57 to 1524 W m^{-2} for adjustment to instrument sensitivity and to measure detector linearity. A photodiode inside the sphere monitors intensity changes.

5. RADIOMETRIC CALIBRATION

Absolute radiometric calibration requires a source of well-known spectral radiance. CHB operates two sources which are certified against German national standard (PTB) for the spectral range 0.35–2.5 µm:

- Integrating sphere (50 cm diameter, 4 x 20 cm² opening). The radiance spectrum and its uncertainty are shown in Figure 4.
- Halogen lamp in combination with a reflectance panel (18 x18 cm²). The uncertainty (k=2) is 2.3 % from 410–1700 nm; it increases towards shorter and longer wavelengths.

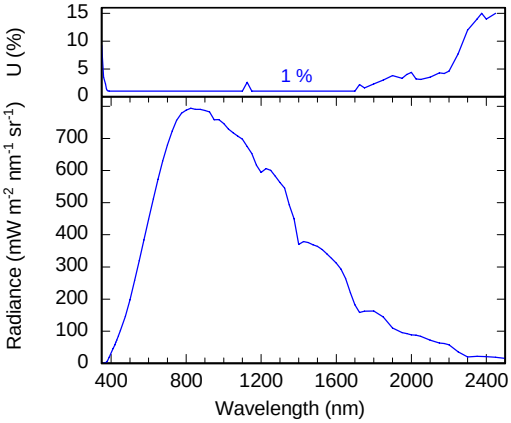

Figure 4. Spectral radiance of small integrating sphere and uncertainty (k=2) according to PTB calibration in November 2007.

Both sources are monitored at each usage by means of a stable spectrometer. If the measured radiance differs at any wavelength in the range 450–900 nm more than 3% from the initial value, the source is re-calibrated at PTB.

6. SPECTRAL MEASUREMENTS

A sensor is spectrally fully characterised by the spectral response functions (SRF) of all detector elements. The SRFs comprise the more convenient parameters centre wavelength, full width at half maximum (FWHM, identical to spectral resolution), spectral sampling distance, and spectral smile (change of centre wavelength across the field of view). To measure a SRF, a spectrally narrow-band beam of radiation is required which overfills both the entrance aperture and instantaneous field of view of the pixel under investigation. Such a beam is provided at CHB by means of a monochromator Oriel MS257. After passing a parabolic mirror (focal length 119 mm) it is reflected at the folding mirror at a well-defined angle to the sensor. The monochromator can be used in CHB for the wavelength range 0.38–14 µm using different gratings. A quartz tungsten halogen (QTH) lamp is used as light source from 380–2500 nm, and a ceramic element from 3–14 µm. Wavelength uncertainty is ±0.15 nm. Spectral bandwidth, beam divergence and geometric cross-section at sensor entrance are set by tuning width and height of the monochromator exit slit. Spectral bandwidth depends further on the selected grating. The minimum spectral bandwidth is 0.1 nm from 0.38–1.4 µm, 0.25 nm from 1.4–3 µm, and 2 nm from 4.5–14 µm. The divergence of the beam is typically 0.8 x 8 mrad², the geometric cross section at sensor entrance in the order of 3 x 4 cm² (at 100 µm slit width, 1 mm slit height).

An example of a spectral measurement is shown in Figure 5 for the sensor ROSIS (Harder 2008). The SRFs of three adjacent channels (no. 27, 28, 29) were determined for the nadir pixel by tuning the monochromator in steps of 0.4 nm at a spectral band width of 0.5 nm (slit width: 150 µm). Since the line shapes are close to Gaussian functions, spectral sensor parameters were determined in this case by Gaussian

fits of the SRF functions. Results were centre wavelength of each channel (495.2, 499.1, 503.1 nm), spectral sampling distances (3.9, 4.0 nm), and FWHMs (6.3, 6.2, 6.2 nm).

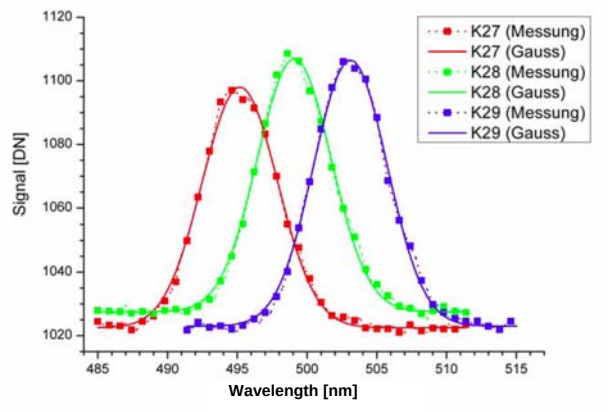

Figure 5: Example of SRF measurements (Harder 2008).

Spectral smile of selected channels was determined by repeating the measurements for several pixels across the field of view. In Figure 6 the centre wavelength of channel 28 is plotted versus the viewing angle: it changes from 498.2 to 501.3 nm, i.e. the change is 3.1 nm (78 % of sampling distance).

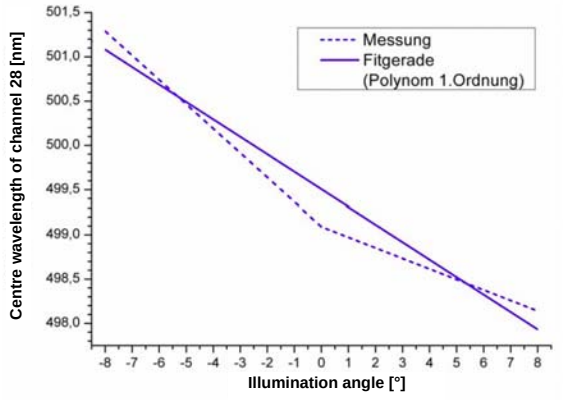

Figure 6: Example of a spectral smile measurement (Harder 2008).

7. GEOMETRIC MEASUREMENTS

The purpose of geometric measurements is to assign angle coordinates to each detector element and to quantify image sharpness by determining the line spread function (LSF). For this, selected sensor pixels are illuminated with spectrally broad-band radiation. A suitable beam is formed at CHB by means of a lamp-slit-collimator combination. Three slits of different width (50, 100, 1000 µm) are mounted tangentially and three identical slits radially on a turnable wheel in the focal plane of a collimator. This set-up produces a beam of well-defined divergence which is parallel to the sensor's along track or across track direction. Due to the collimator's focal length of 750 mm the beam divergence is 0.067, 0.13 or 1.3 mrad in its narrow direction. The geometric cross section is 12 cm. The beam is reflected to the sensor at a well-defined angle by means of the folding mirror. For typical sensors the beam with 0.067 mrad illuminates a fraction of a pixel, while the beam with 1.3 mrad overfills the pixel. During a measurement the incident angle is changed in small intervals either by stepping the folding mirror (minimum increment 0.0017 mrad) or the slit wheel (0.0076 mrad).

Figure 7 shows an example of a LSF measurement (Suhr 2008). The measurement was performed for the nadir pixel (no. 192) of the imaging spectrometer AISA. The tangentially mounted 50 µm slit was used as calibration target. Since it was illuminated by a broad-band light source, all channels of pixel 192 receive light, i.e. a narrow 'line of light' is projected to the focal plane. This line was moved across the pixel by turning the folding mirror in steps of 0.01°. The normalised signals of 5 channels are shown as a function of the incident angle. These functions are called line spread functions (LSF). The centroid of a detector element's LSF is its across track viewing angle, its FWHM the geometric resolution across track. The LSF's Fourier transform is the modulation transfer function (MTF).

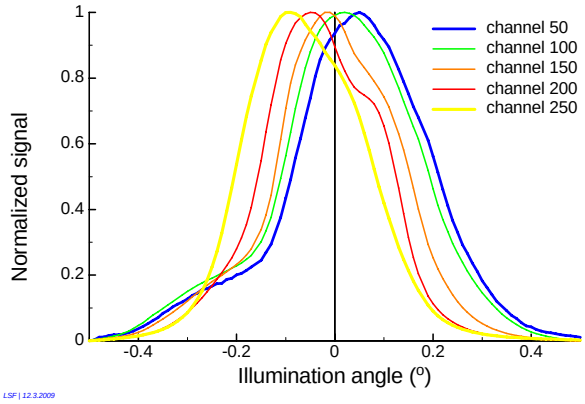

Figure 7: Example of LSF measurements (adapted from Suhr 2008).

8. AUXILIARY MEASUREMENTS

The above-mentioned measurements are relevant to determine basic parameters required for calibration of optical sensors. Calibration can be improved using auxiliary measurements of the following instrument properties:

- *Detector linearity:* radiation is attenuated in well-defined steps using neutral density filters.
- *Spectral stray light:* spectral filters block radiation in well-defined spectral intervals. Sensor signals in these regions are caused by stray light inside the instrument.
- *Spatial stray light:* selected pixels are illuminated using the set-up for geometric measurements. Signals of non-illuminated pixels are caused by stray light inside the instrument.
- *Polarisation sensitivity:* a set of 3 linear polarisers is available to characterise the dependency of sensor response on polarisation from 0.47–2.5 µm.

Calibration can be checked by measuring the radiance of coloured reflectance panels which are illuminated by a calibrated halogen lamp.

An example of spectral stray light measurements is shown in Figure 8 (Damm 2007). The measurements were performed for the hyperspectral sensor ROSIS using 10 band pass filters which transmit radiation in narrow spectral intervals.

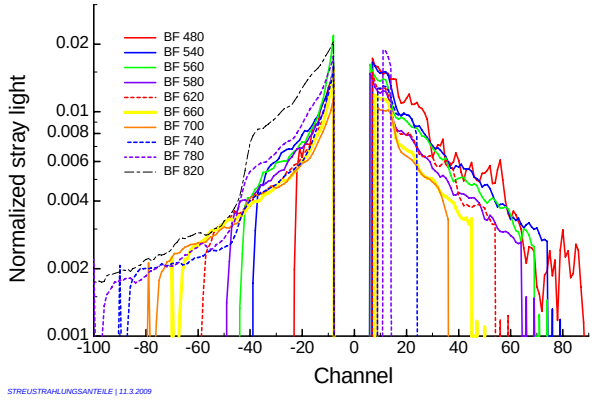

Figure 8: Example of spectral stray light measurements (adapted from Damm 2007).

The filters were illuminated in transmission using CHB's small integrating sphere. The plots of Figure 8 show signals measured in non-illuminated channels, normalised to the integral signals of all nominally illuminated channels, and shifted spectrally such that the centre wavelength of each filter is assigned to the virtual channel no 0. Hence, the gap around channel 0 corresponds to the spectral region in which the filters transmit radiation, and the curves to the left and to the right of the gap quantify spectral stray light relative to the integral signal. The curves are very similar for all filters, i.e. spectral stray light can be approximated for this sensor by a unique function which only depends on wavelength differences, but not on the wavelength itself. This function is the average of the shown curves. Using this function, the stray light can be estimated for any radiance spectrum. Figure 9 shows such an estimate.

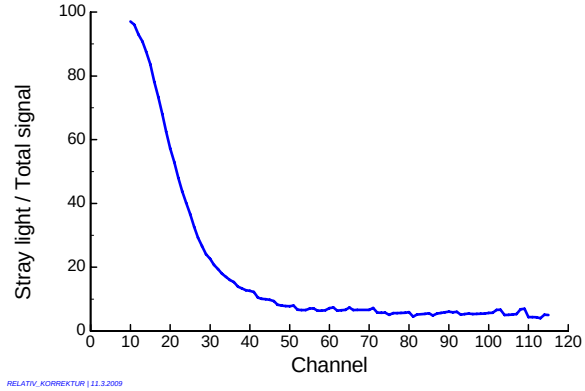

Figure 9: Estimate of spectral stray light at radiometric calibration (adapted from Damm 2007).

The curve of Figure 9 represents a measurement of CHB's small integrating sphere as used routinely for radiometric calibration. It shows that > 5 % of the signal is caused by stray light. Very critical is the strong increase below channel 50. If not corrected, stray light during laboratory calibration causes for this sensor significant overestimation of the response for $\lambda < 550$ nm (Lenhard et al. 2009). The necessity of stray light correction is not specific for this sensor; for example, the atmosphere correction algorithm of SeaWiFS (Gordon 1995) explicitely accounts for stray light, which is in the order of 9 % for channel 8 (845–885 nm).

9. COMPUTER CONTROL

Since a full measurement cycle may last many hours or even some days, major CHB components are computer controlled, and time-consuming steps can be done automatically without operator interaction. The flow-chart of the software is shown in Figure 10.

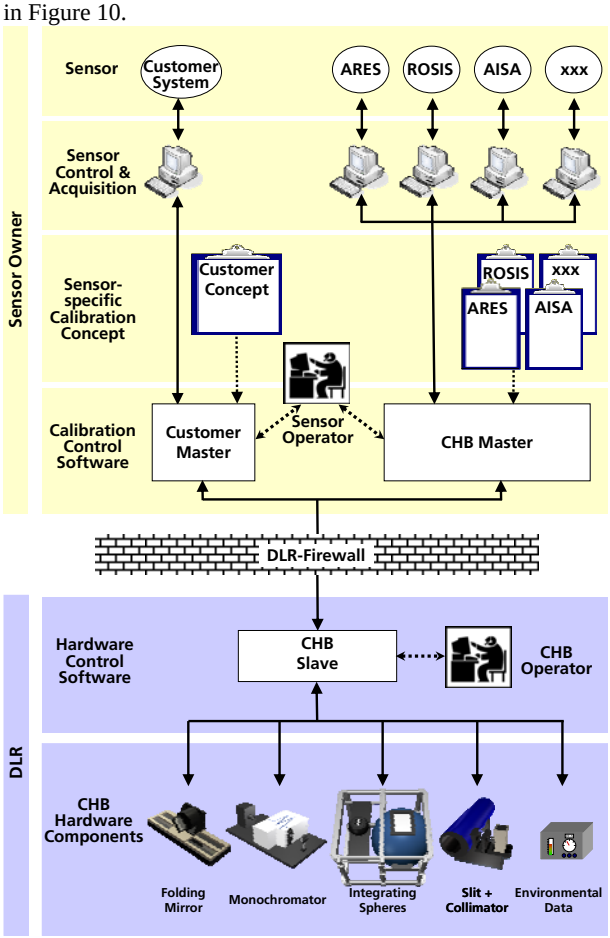

Figure 10: Flow-chart of CHB software.

Two software packages enable automated measurements:

- *CHB Slave*. Controls CHB devices.
- *CHB Master*. Implements the measurement concept, commands both the CHB slave software and the sensor software. Can be adapted to any sensor that supports external control by XML commands.

To control the CHB devices via the CHB Master, a set of about 60 parameters is used. This set includes device-groups for the sensor, folding mirror, monochromator, collimator and integrating sphere.

10. SERVICES

CHB is accessible to customers on request. DLR staff is available to adapt the customer's instrument mechanically to CHB, set-up its communication with CHB Master software, operate CHB hardware and software, assist the measurements, and support in data interpretation.

11. SUMMARY

A new facility designed to perform calibration measurements of airborne imaging spectrometers was established at the German Aerospace Center (DLR) Oberpfaffenhofen. It will be kept operational for a period of at least 5 years for the calibration of APEX. Besides that, it will be continuously upgraded to meet the requirements of other sensors, in particular of DLR's own airborne imaging spectrometers (e.g. ROSIS, upcoming ARES) and field spectrometers.

ACKNOWLEDGEMENTS

The authors would like to thank M. Damm, M. Goubeau, S. Harder and M. Kuhlbach for their contributions to the improvement of CHB by adapting and testing ROSIS and AISA, and for providing results of their Diploma theses to this article. R. Brankatschk, M. Ecker and S. Leistenschneider are acknowledged for developing parts of the software. Valuable support was given by the APEX team, in particular by E. Alberti, F. Dell' Endice, K. Itten and J. Nieke. Essential parts of the infrastructure described above were funded by ESA under contract 16586/02/NL/GS.

REFERENCES

Damm, M. 2007. Charakterisierung und Korrektur von Streulicht in einem flugzeuggetragenen Hyperspektralsystem. Diplomarbeit, University of Applied Sciences Mittweida, 117 pp. (Unpublished results)

Gege, P., Fries, J., Haschberger, P., Schötz, P., Schwarzer, H., Strobl, P., Suhr, B., Ulbrich, G., Vreeling, W. J. 2009. Calibration facility for airborne imaging spectrometers. *ISPRS Journal of Photogrammetry and Remote Sensing (in press);* doi: 10.1016/j.isprsjprs.2009.01.006

Gordon, H. R. 1995. Remote sensing of ocean color: A methodology for dealing with broad spectral bands and significant out-of-band response. *Appl. Optics* 34, 8363-8374.

Harder, S. 2008. Implementierung des Hyperspektralsensors ROSIS in ein neues Kalibrierlabor. Diplomarbeit, TU München, 123 pp. (Unpublished results)

Itten, K. I., Dell'Endice, F., Hueni, A., Kneubühler, M., Schläpfer, D., Odermatt, D., Seidel, F., Huber, S., Schopfer, J., Kellenberger, T., Bühler, Y., D'Odorico, P., Nieke, J., Alberti, E., Meuleman, K., 2008. APEX - the Hyperspectral ESA Airborne Prism Experiment. *Sensors*, 8, 6235-6259; doi:10.3390/s8106235

Kuhlbach, M. 2008. Weiterentwicklung des Hyperspektral-sensors AISA für den Feldeinsatz. Diplomarbeit, Munich University of Applied Sciences, 87 pp. (Unpublished results)

Lenhard, K., Damm, M., Gege, P. 2009. Effects of spatial and spectral stray light on radiometric calibration of a hyperspectral pushbroom sensor. *Proc. 6th EARSeL SIG IS Workshop, March 16-18, 2009, Tel Aviv, Israel. (This CD-ROM)*

Suhr, B. 2009. Sensor independent concept for characteri-sation of hyperspectral imaging spectrometers. Dissertation, Univ. Zürich. (In preparation)